MINERALOGICAL AND CHEMICAL CHARACTERIZATION OF SENSOR-BASED SORTED COPPER ORES

Supported by tetfund TERTIARY EDUCATION TRUST FUND

A. I. Ambo[1,2]* and H. J. Glass[1]
[1]Camborne School of Mines, University of Exeter, Penryn TR10 9EZ, Cornwall, UK
[2]Department of Chemistry, Federal University of Lafia, Nigeria
*Corresponding author: amboamosidzi@yahoo.com

Received: January 29, 2020 **Accepted:** February 25, 2020

Abstract: Near infrared sensor-based pre-concentrated copper ores were characterized quantitatively and qualitatively for mineralogical and chemical composition using optical microscopy and mineralogical methods (QEMSCAN®, X-ray diffraction (XRD), scanning electron microscopy (SEM) and geochemical methods (X-ray fluorescence spectrometer (PXRF) and Inductively Coupled Plasma Mass Spectrometry (ICP-MS).The investigation was carried out towards understanding the satisfactory copper recovery methods based on copper grade. The analysis was done according to the ore category: product, middling and waste. Result obtained showed that the ore contained different minerals and metals in variable concentration according to the ore categories. Chrysocolla was determined to be the dominant copper ore mineral. The elemental concentration of the metals indicated a different pattern which is attributed to the increase in surface area and the analytical technique used. However, a strong correlation between the different analytical techniques was found. This suggests good correlation in the method of analysis. This work revealed the potentials of the application of an automated technique of ore pre-concentration for processing of ore minerals on the basis of mineralogical and chemical content.

Keywords: Copper, sensor-base, sorting, minerals, pre-concentration, near infrared

Introduction

Copper, in various forms, has been mined from the Earth ever since mankind started using metal tools. Today, rich copper deposits are scarce and deposits of native copper (pure copper metal) are very rare (Baba *et al*., 2013). Most ores mined today contained copper in complex assembly of minerals; with the ore matrix made up of compounds that contain less than 1% copper (Amos *et al.*, 2020). This Complex copper ore minerals are increasingly expensive to process and require detailed analysis of the ore component to establish the most viable techniques and methods for recovering copper (Amos *et al.*, 2017; Amos *et al.*, 2020). The ore analysis is usually focused on the evaluation of mineralogy and associated gangue present in order to mitigate unwanted processing cost (Neighbour, 2010). This is because mining of the ore at times does not pose much problem unlike the processing to obtain copper and other valuable metals which could be complicated due to the complex nature of the ores (Oscar *et al*., 2019). In recent times several strategies and approach that will lead to efficient recovery of minerals from the ore matrix are usually adopted. The key objective is the discrimination of unwanted materials and gangue through pre-concentration before subjecting the ore to further processing (Iyakwari and Glass, 2016; Amos *et al.*, 2020). Understanding the mineralogical and chemical composition and properties of such ores is important in determining its processing method (Liu *et al.*, 2010; Biswas and Davenport, 2013; Iyakwari *et al.*, 2016; Whiteman *et al.*, 2016). The analysis may require liberation of the mineral from its host rock before subjecting such to different methods of instrumental technique. While it is well known that the mineralogy and texture of ore rock could influence its mineral processing behavior (Neighbour, 2010), method for the quantified measurement and characterization of mineralogical and chemical constituent can be used to predict variability in the composition which in turn results in effective mineral processing (Helle *et al.*, 2005; Neighbour, 2010; Anderson, *et al.*, 2009; Kalichini *et al.*, 2017). An absolute, dependable method of quantitative analysis is important in order to effectively determine the composition of the ore (Little, 2018). Various methods, which include chemical, physical and mineralogical have been used (Anderson *et al.*, 2009). It has been shown that no single method is sufficient due to susceptibility of the instrument to factors such as detection limit which may vitiate the results (Queralt, 2005). In most cases a combination of different methods of analyses are adopted (Helaluddin, 2016). For instance, X-ray Diffraction has been found to be effective method of quantitative determination of copper ores due to its ability to detect the minerals and chemical combination present in the ores (Queralt, 2005; Reed, 2005; Zhou *et al.*, 2018). The QEMSCAN® instrument has been effectively deployed for rapid mineralogical assessment, including the spatial mapping of minerals (Gottlieb *et al.*, 2000; Pirrie and Rollinson, 2011). Scanning electron microscopes commonly have an X-ray spectrometer attached, enabling the characteristic X-rays of a selected element to be used to produce an image. The advantages of the SEM as an imaging instrument (high spatial resolution, large depth of field, and simple specimen preparation) make it an invaluable tool in determining the mineralogy of an ore. X-ray fluorescence (XRF) analysis has been a standard method of elemental analysis in geology for a long time and offers good accuracy for major elements and detection limits in the region of 1 ppm (Reed, 2005; El-Taher, 2012).

Sensor-based technique for ore sorting is now popular and is gaining acceptance in mineral processing; it is a method of ore pre-concentration where singular particles are individually analysed and mechanically separated based on physical properties after determining these properties by a sensor (Pirrie and Rollinson, 2011; Dalm *et al.*, 2014). The technology has a lot of potentials in the mining industry because it can be applied on relatively coarse ore particles, beside that it allows for the incorporation of the technique as a pre-concentration step in ore processing operations (Sabins, 1999; Wotruba and Riedel, 2005). The application of this technique is aimed at eliminating waste or sub-economic material prior to the conventional concentrating methods (Dalm *et al.*, 2014). Different sensor types that are currently used with sensor based sorting include optical, near infrared, X-ray transmission and electromagnetic sensors.

The near-infrared (NIR) sensor has been proven to be a valuable tool in mapping the distribution of mineral alterations in hydrothermal ore deposits and in pre-concentrating porphyry Cu ores deposits (Salter and Wyatt, 1991; Sabins, 1999; Thompson *et al.*, 1999; Wotruba *et al.*, 2009). The use of the technology in ore sorting operation is becoming famous due to dwindling ore resources and its versatility and application in mineral processing. The

principal attractiveness of the technique isits direct and non-invasive nature, as the main driving force towards efficient and sustainable ore pre-concentration. The technique can be used for quantitative application targeted at determining major constituents in ore samples and for some specific applications under favorable characteristics of the sample matrix. Also, for qualitative application for identification and classification of samples by assigning each spectrum in the spectral set used for training the identification/classification algorithm attributed to a given class of ores (Celio, 2003).

In this current study, complex copper ore samples of hydrothermal origin were pre-concentrated using near infrared sensor based technique and the ore classified into three different categories based on copper grade. The ore fractions were further characterized for mineralogical variation and chemical content across different ore category using different technique to establish effective copper processing and to improve the understanding of the elemental distribution in the ores.

Materials and Methods

Copper ore samples were obtained from Montverde mine operations in Los pozos mining district in the coastal Range of the Atacama Region, Northern Chile. A total of 32 samples (size between 5 and 10 cm) were considered for pre-concentration (Amos *et al.,* 2020) and mineralogical/chemical characterization. For particle size fraction analysis, the classified ore particles were crushed separately with a Retsch steel jaw crusher (to -3 mm), milled, homogenised and then sieved to obtained the following size fractions: -125/+90, -90/+63 and -63/+45 µm.

Ore pre-concentration

The ore was pre-concentrated using Near InfraRed (NIR) sensor-based technique in Camborne School of Mines, University of Exeter, United Kingdom. The NIR line scanner at Camborne School of Mines (CSM) measures each spectrum at a dimension of 0.29 by 0.9 cm. Each sample was an average of between 2 and 2.7 cm. In order to properly map each sample, individual samples were divided into three sectors measuring 0.9 cm each, corresponding to NIR spectrum height, with width measuring 0.29 cm (Fig. 1). The number of spectra produced by individual samples per sector depended on particle size and shape. The NIR pre-concentration strategy employed is aimed at eliminating both calcite and clay (muscovite/kaolinite) rich particles as gangue. Hence, samples were classified as product, middling or waste based on the amount of copper content according to the method described by (Iyakwari *et al.,* 2016; Amos *et al.,* 2020). It should be noted that the NIR examine minerals based on their functional group(s), in this case (calcite, ankerite, malachite, muscovite, kaolinite, biotite, chrysocolla, malachite, chlorite, tourmaline and apatite) minerals were determined.

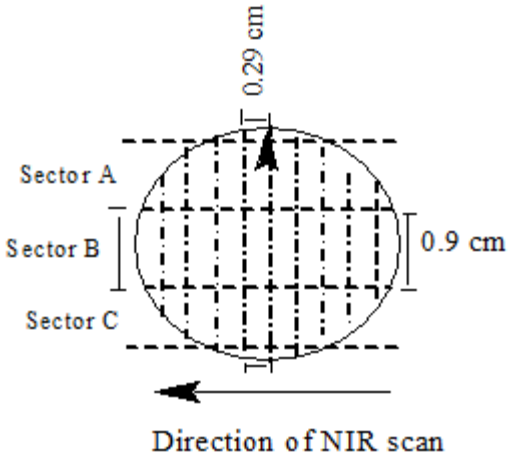

Fig. 1: Samples marked for directional scanning and spectra/mineral mapping (after Iyakwari *et al.*, 2016)

Samples NIR spectral correlation and interpretation

The NIR strategy employed was targeted at eliminating both calcite and clay (muscovite/kaolinite) rich particles as gangue (Iyakwari *et al.,* 2016). Hence, samples were classified into three groups as:

i. Product - the samples with all NIR spectra showing chrysocolla and or hematite, chlorite, biotite pattern. This group includes featureless NIR spectra.
ii. Waste - the samples with all NIR spectra showing calcite and or muscovite characteristic spectra.
iii. Middling – the samples with NIR spectra containing individual spectra of both waste and product groups. This is likely since individual mineral grains are smaller than the pixel size of 2.9 by 9 mm, and particles scanned consisted of at least two pixels (which may be distinct). This group may require further liberation to a size not less than the pixel size and rescanned.

Individual sample NIR spectra mapping

Three representative samples from each class (Figs. 2, 3 and 4) representing products, middling and waste respectively are described here in detail. Major absorption features, absorption wavelength position, correlation with reference spectra, and the possible mineral(s) responsible for the absorption features are correlated with mineral data and field scan images.

Product sample generated a total of 22 NIR spectra, corresponding to 8, 8, and 6 spectra per sector scanned (Fig. 2(a, b and c)). Spectra display no absorption feature(s).

A total of 26 spectra were generated from scan of middling sample (Fig. 3(a, b and c)). Spectra of sectors A and B displayed no features, while spectra of sector C shows strong mineralogical variation with spectrum number 1, 2, 3, and 4 showing no absorption features, while spectrum number 5, 6, 7, 8 and 9 all showed features near 1410, and 2200 nm. The features displaying spectra also exhibited relatively higher reflectance compared to those without features. The position of features near 1410 and 2200 nm corresponds to muscovite features (Iyakwari *et al.,* 2013; Iyakwari, 2014; Iyakwari *et al.,* 2016). The featureless spectra correspond to hematite dominated spectra. Muscovite displays diagnostic absorption features in spectrum number 5, 6, 7, 8, and 9. This indicates that muscovite is concentrated more around those spectra. This is confirmed by the sample NIR-active minerals field scan image (Fig. 3d). The sample field scan image also reveals that the sample has a porphyritic texture, showing a highly zoned concentration of hematite with patches of muscovite to the lower left of the image.

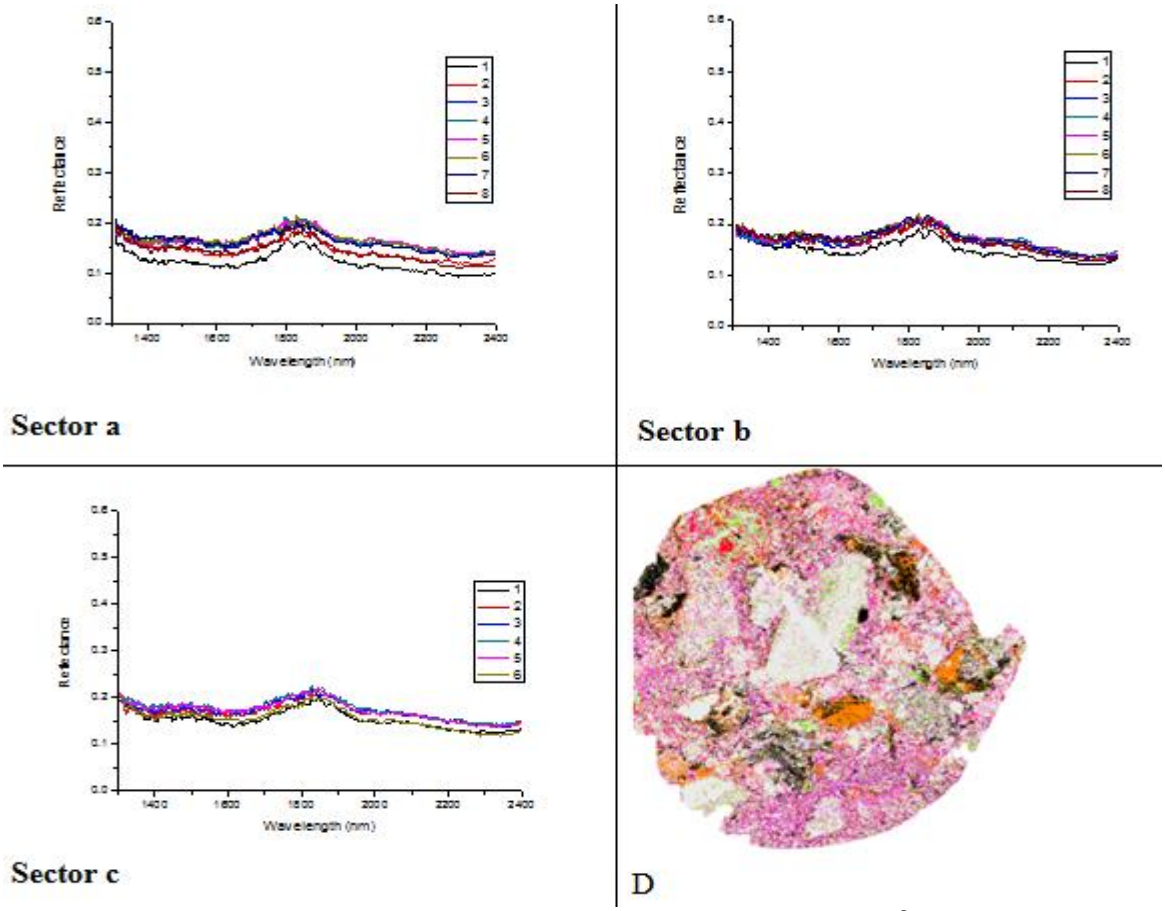

Fig. 2: (sectors a, b and c) –NIR spectra of product sample While d is the QEMSCAN® fieldscan image of sample at 10 µm X-ray resolution, showing only NIR active minerals present in the sample

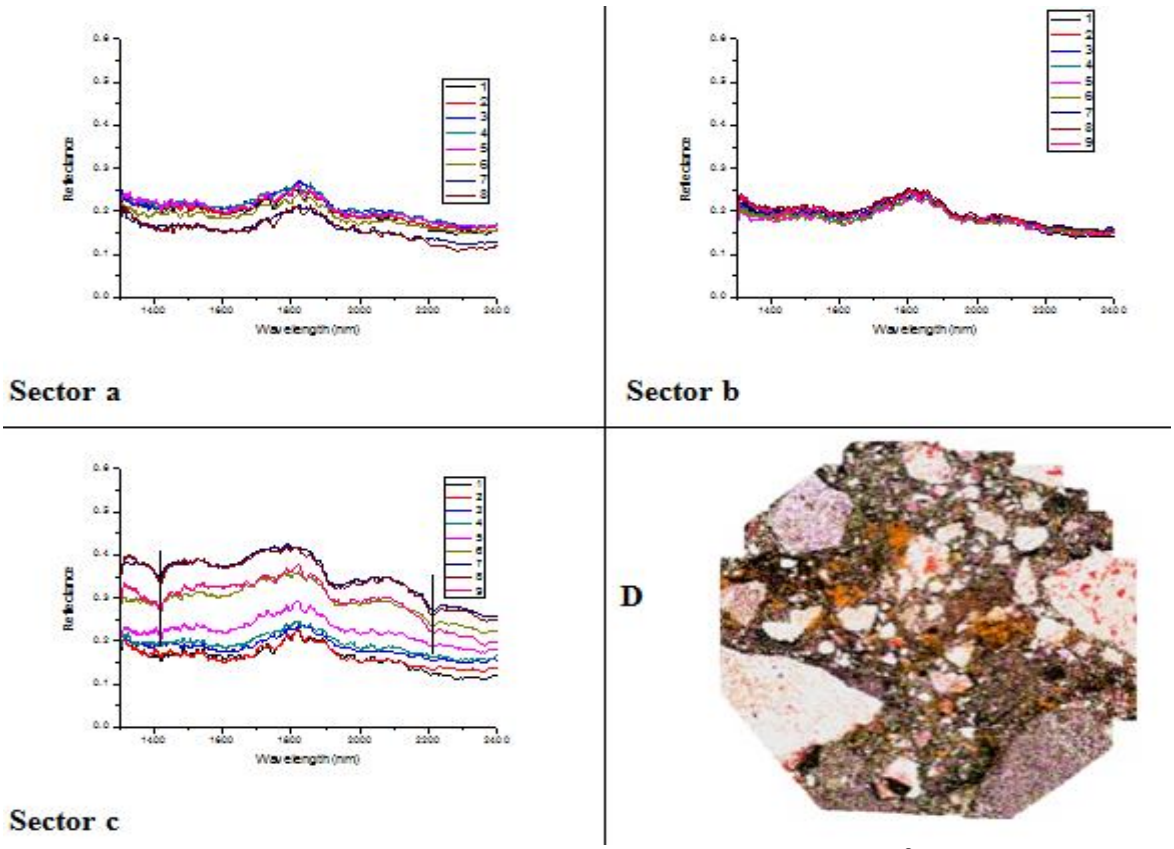

Fig. 3: (sectors a, b and c) –NIR spectra of middling sample. While d is the QEMSCAN® fieldscan image of sample at 10 µm X-ray resolution, showing only NIR active minerals present in the sample

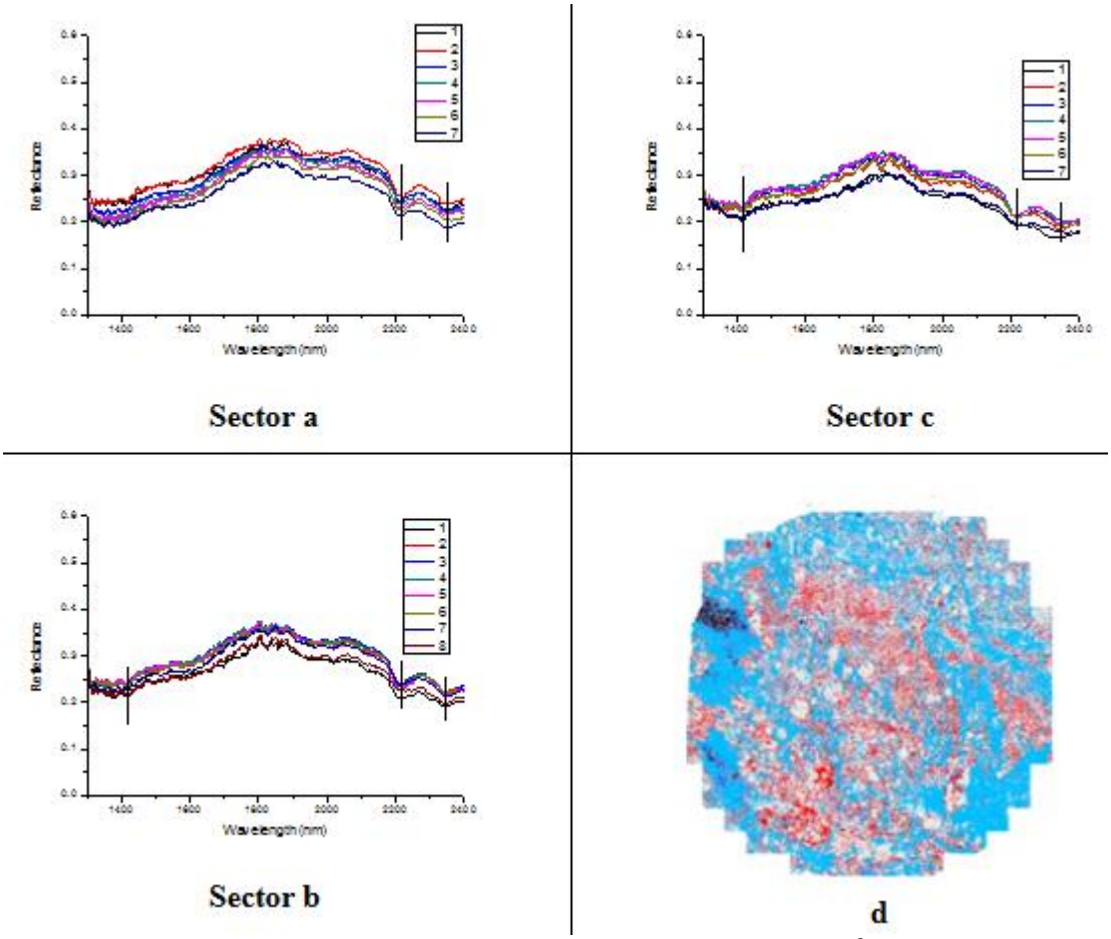

Fig. 4: (sectors a, b and c) NIR spectra of waste sample. While d is the QEMSCAN® fieldscan image of sample at 10 µm X-ray resolution, showing only NIR active minerals present in the sample

Spectra of waste sample (Fig. 4 (a, b and c)), display characteristic muscovite and calcite features near 1415, 2210 and 2345 nm. Spectra also display high reflectance, which is indicative of absence or low hematite concentration in the sample. A total of 22 spectra were generated from the scan corresponding to 7, 8 and 7 spectra per sector (Amos *et al*., 2020).

NIR-active minerals field scan image of sample (Fig. 4d) show both calcite and muscovite occurring almost in same space and time.

Mineralogical analysis

The mineralogical analysis of the pre-concentrated copper ore (product, middling and waste) was carried out with QEMSCAN® 4300 system, which is based on a Zeiss scanning electron microscope.

A Siemens Bruker D500 XRD analyser (www.bruker.com) with a detection limit of 5% was used to semi-quantitatively measure the mineralogical composition of the ore. Samples to be determined were prepared as epoxy resin mounts with Epofix resin and polished to a 1 µm finish before carbon coating. Each sample, having an average size of between 2 and 2.7 cm, was mapped using the field scan measurement mode in order to obtain a full image of the sample being measured. XRD measurements were matched with known mineral signatures using Bruker EVA software. The patterns generated by the XRD scan were smoothed before interpreted using the JCPDS PDF-2 (2004) database.

Chemical/textural analysis

Elemental composition of the classified ore samples was measured using portable desktop thermo scientific Niton FXL 950 FM X-Ray Fluorescence analyser (XRF, www.nitonuk.co.uk). The portable XRF (PXRF) analyser employs Energy Dispersive Spectrometry (EDX) method. The measuring window covers a diameter of 8 mm, and X-rays penetrates approximately 1 to 2 mm into the sample.

Scanning Electron Microscope (SEM) was used to observe ore characteristics such as texture, size and liberation sizes in relation to copper. Polished blocks of-63/+45 µm samples were coated with carbon to improve imagery and enhance surface conductivity. The SEM equipment used for the analyses was a JEOL JSM-5300LV Low Vacuum SEM equipped with EDS ISIS software.

The metal grades of the pre-concentrated and classified ore were determined with Inductively Coupled Mass Spectroscopy (ICP-MS, Agilent Technology, Model 7700). Samples were first digested by dissolving the fractions in Aqua regia (75% 6N HCl and 25% 15.8N HNO_3) at 90 ˚C for 1 h. 50 times dilution of leachate was carried out with 50% HNO_3 prior to determination with ICP-MS. Experimental results obtained revealed that the ICP-MS produces very good precision with variability of 1.2% between sample batches with a maximum standard deviation of 0.1% for the metals determined. The outline flowchart for the analysis is shown in Figure.

Results and Discussion

Quantitative and qualitative analyses were carried out according to the instrumental techniques described in Fig. 5. Data obtained from the analysis showed contrasting results. X-ray diffraction analysis of the mineralogical composition of the pre-concentrated ore indicated the presence of some major minerals which include: quartz, hematite, clinochlore

(chlorite), orthoclase and microcline (K-feldspar), muscovite, calcite and biotite as the eight dominant crystalline mineral constituents. The XRD pattern for the product, middling and waste classified ore are shown in Figs. 6, 7 and 8. The figures exemplified typical profiles of the pre-concentrated ore obtained. The observed rise in baseline confirms the presence of the amorphous mineral (chrysocolla), which is in line with (Gaydon, 2011; Iyakwari, 2014) on rise of baseline of XRD pattern with increase in the 2-theta value suggesting the presence of chrysocolla as the dominant amorphous mineral in an ore.

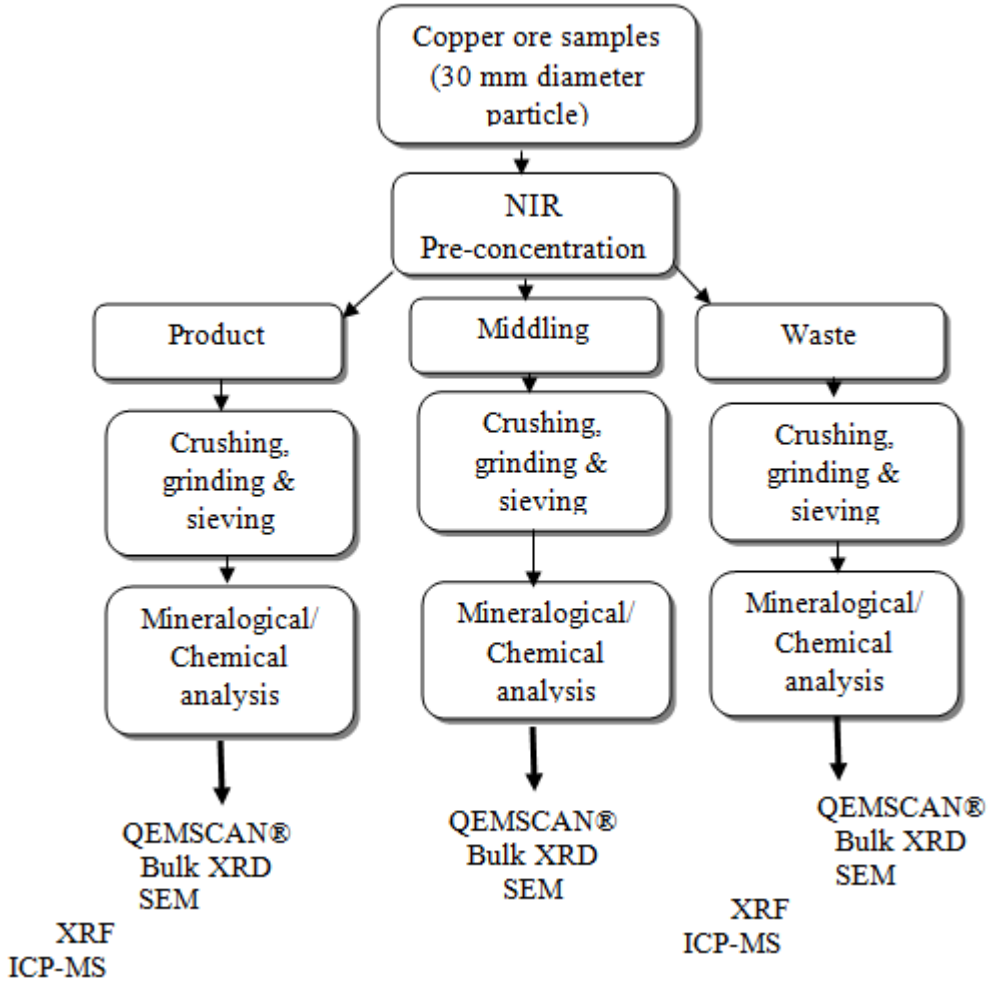

Fig. 5: Outline strategy of ore pre-concentration and mineralogical/chemical analysis

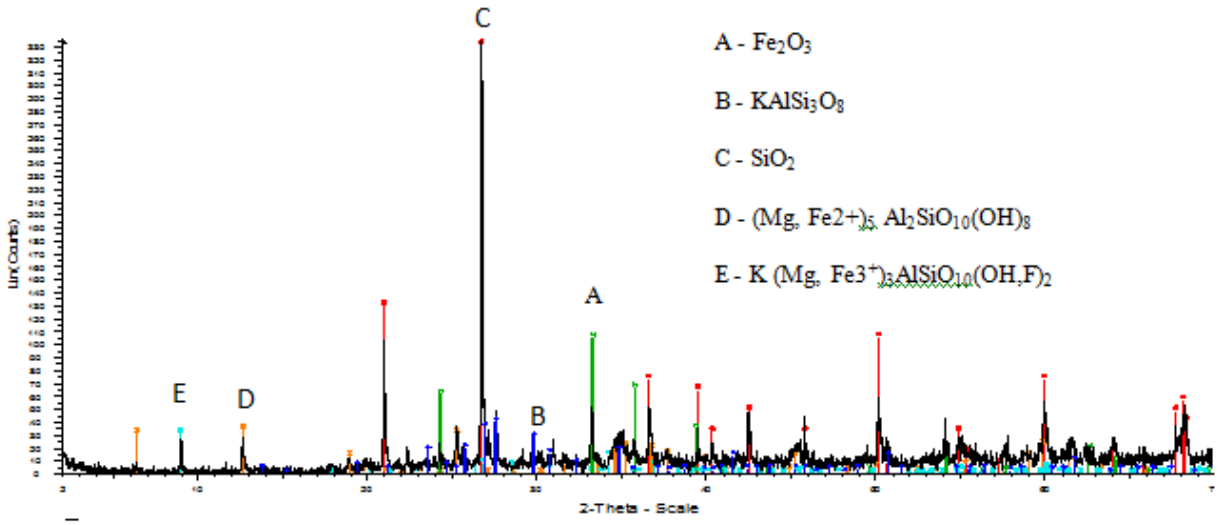

Fig. 6: XRD profile of bulk product sample

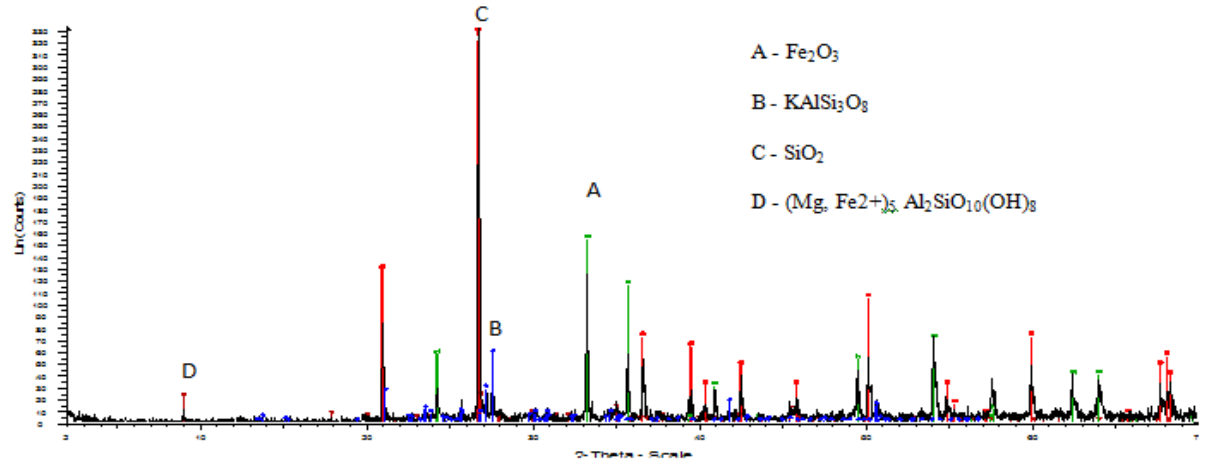

Fig. 7: XRD profile of bulk middling sample

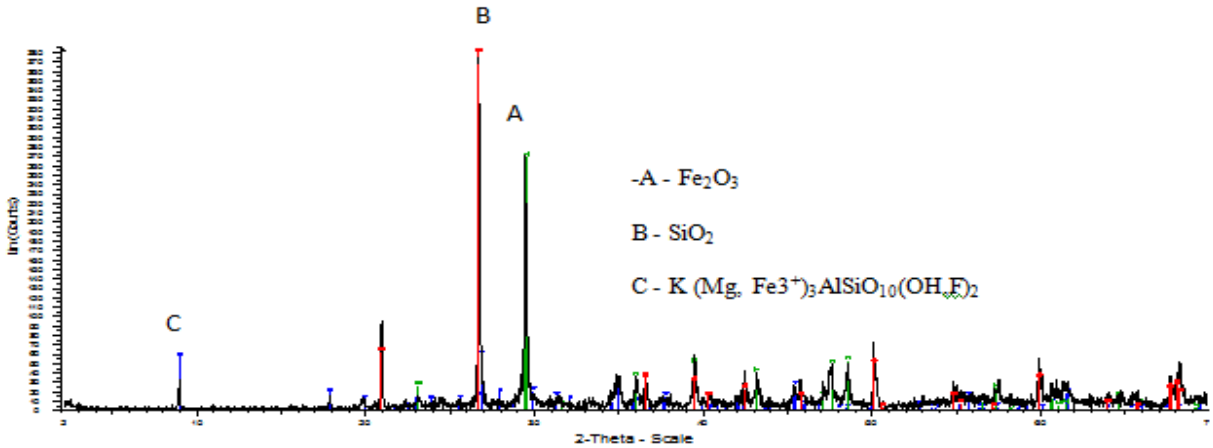

Fig. 8: XRD profile of bulk waste sample

XRD detection limit is 5%, the technique cannot be used to determine trace minerals in the ore. Because of this QEMCAN® was used to identify much wider range of minor minerals that are below the detection limit of the XRD equipment. Mineralogical analysis by this instrument revealed that the ore contained different minerals (Table 1).

Table 1: Minerals present in the classified ore

No.	List of minerals	Chemical formula
1	Chrysocolla	$(Cu, Al)_2H_2Si_2O_5(OH)_4.n(H_2O)$
2	Cuprite	Cu_2O
3	Malachite	$Cu_2(CO_3)(OH)_2$
4	Biotite	$K(Mg,Fe)_3(AlSi_3O_{10})(F,OH)_2$
5	Ankerite	$Ca(Fe,Mg,Mn)(CO_3)_2$
6	Hematite	Fe_2O_3
7	Calcite	$CaCO_3$
8	Muscovite	$KAl_2(Si_3Al)O_{10}(OH,F)_2$
9	Kaolinite	Al_2O_3 $2SiO_2{\cdot}2H_2O$
10	Chlorite	(Mg,Fe)3(Si,Al4O10(OH)2·(Mg,Fe)3(OH)6
11	Quartz	SiO_2
12	Plagioclase	$(Na,Ca)(Si,Al)_4O_8$
13	K-feldspars	$KAlSi_3O_8$
14	Tourmaline	$NaFe^{3+}{}_3(Al_4Mg_2)Si_6O_{18}(BO_3)_3(OH)_3O$
15	Apatite	$Ca_5(PO_4)_3(OH,F,Cl)$

QEMSCAN® modal mineral data showed that, of the three copper-bearing minerals present, chrysocolla constitutes about 94.4 wt. % and malachite and cuprite 5.3 wt. % and 0.4 wt. %, respectively. Other associated minerals are present at variable concentration. The minerals containing iron are hematite, ilmenite, biotite and ankerite with hematite and biotite been the most common in the pre-concentrated and classified ore.

The cumulative mineral data of each ore category (product, middling and waste) is presented in Table 2. The result in the Table is a reflection of the total concentration of each mineral in the classified ore. Cumulative values (wt. %) obtained infer that the concentration of copper is product > middling > waste.

The pattern of some mineral concentration (chrysocolla and K-feldspar) followed a systematic order from product to middling to waste. The inverse pattern, where the waste ranked higher than the middling and product, was observed for muscovite, and ankerite.

A different pattern, where the waste, middling or product ranked high in certain minerals was observed for kaolinite, biotite, tourmaline, chlorite, plagioclase, cuprite, malachite, calcite, quartz and apatite. Amongst all the minerals, apart from chrysocolla, the cumulative values of muscovite, biotite, chlorite, quartz, K-feldspar, hematite, and calcite were well above 1.3 wt. % in the pre-concentrated ore samples. However, K-feldspar, chlorite, quartz, and hematite all have significantly higher values than the rest of the minerals in the ore.

Scanning Electron Microscopy (SEM) was used to characterize the ores samples. The elemental composition of the ore was determined in each case. The instrument was alsoused to observe the ore characteristics such as texture, size, shape and liberation sizes in relation to copper. It was found that the Cu is interlocked with other metals in the ore matrix (Fig. 9). Results obtained for the pre-concentrated ore samples were similar where copper particles in the crushed ore are finely disseminated; the ore is morphologically characterized by intergrowth with chrysocolla minerals

hosting copper particles residing within the hematite rich iron source and K-feldspars. This was also observed from the QEMSCAN® images shown in Figs. 2 – 4. The only difference between the three classes of the ore was in the concentration of elements as shown in Table 3. The observed phenomenon could be due to absorption of elements by chrysocolla as shown in the spatial variability within the crushed ore with copper ubiquitously distributed within the crushed grain matrix containing chrysocolla, K-feldspar and hematite.

It should be noted that for the waste, abundant peaks of some elements (Fe, Mg, Si) that correlates with results in Table 2 for the corresponding minerals hosting them was observed. For the middling very abundant peaks of Fe with short peaks of Cu peak were obtained with corresponding elements (Al, Si, K, Ca), while for the product polished blocks the Cu peak was very pronounced compared to the former. Although, the Fe peaks were more pronounced, the observed peak heights were not like that in the middling. In all the samples investigated the observed peaks appear to correlate with their mineralogical concentrations according to the classification. The SEM image in Fig. 9 revealed typical distribution of minerals within the ore matrix with copper in close association with hematite and K-feldspars finely disseminated in the ore.

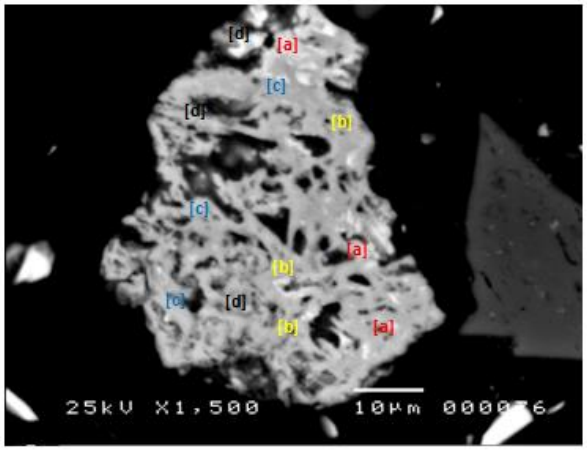

Fig. 9: BEI SEM image of polished block. [a] Cu, $Al)_2H_2Si_2O_5(OH)_4.n(H_2O$, [b] Fe_2O_3, [c] $KAlSi_3O_8$, [d] SiO_2

Table 2: Cumulative mineral data for product, middling and waste samples (wt. %)

NIR Classification	Silicates									Oxides			Carbonates	Phosphates	Others (Trace phases)	Total
	Cu-bearing	Non-Cu-bearing								Cu-bearing	Non-Cu-bearing					
	Non-Iron-bearing			Iron-bearing		Non-Iron-bearing				Iron-bearing	Non-Iron-bearing		Iron-bearing	Non-Iron-bearing		
	Chry-socolla	Musco-vite	Kao-linite	Bio-tite	Tour-maline	Chlo-rite	Quar tz	K-feldspar	Plag-feldspar	Hem-atite	Cup-rite	Mala-chite	Calci te	Ankerite	Apatite		
Products	7.95	2.86	0.08	9.36	0.32	9.36	14.77	23.20	0.17	28.58	0.02	0.32	1.91	0.34	0.20	0.57	**100**
Mid-dlings	4.36	3.07	0.49	5.10	0.73	6.14	14.71	15.75	0.31	47.35	0.00	0.00	1.30	0.52	0.00	0.20	**100**
Waste	0.68	3.75	0.01	7.33	0.45	21.54	34.85	14.35	1.07	1.65	0.01	0.15	11.49	0.62	0.35	1.70	**100**

Table 3: Metals and metal oxides analysis of pre-concentrated ore (product and middling) with SEM (wt. %)

Metal concentration ↓ Sample category→	Product	Middling	Metal Oxides↓ Category →	Product	Middling
Na	0.13	0.13	Na_2O	0.18	0.18
Mg	0.60	0.10	Mg_2O	0.99	0.17
Al	0.21	0.12	Al_2O_3	0.40	0.23
Si	12.10	12.22	SiO_3	26.1	26.14
K	6.18	0.26	K_2O	7.45	0.31
Ca	1.71	0.71	CaO	2.39	0.99
Fe	40.0	48.11	Fe_2O_3	57.19	68.78
Cu	4.23	4.01	CuO	5.30	3.20

The relative abundance's of elements in the samples were determined from their metal oxides (Table 3). In each case the determination was carried out in triplicate and averages taken. The values obtained are only qualitative and are based on standard-less analysis, and in each case the values normalized to equal 100%. The determination is based on elements requested on a point location and identified by the SEM. As such the possibility of other elements occurring in appreciable amount which could be measured cannot be ruled out.

A correlation plot (Fig. 10) for the metal oxides investigated by SEM showed a slight variation in the concentration between the two ore categories determined. This suggests a good correlation of analysis as indicated by the difference in mineralogical composition as a result of the sensor-based sorting of the ore.

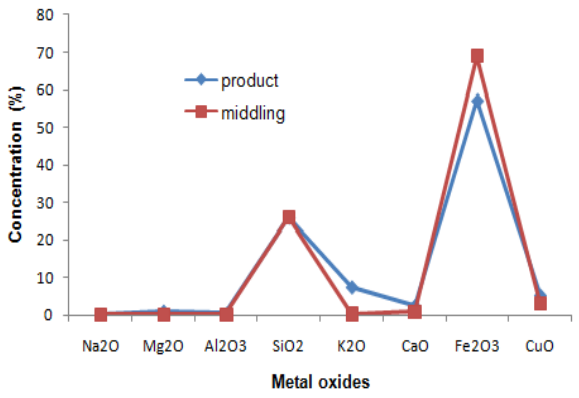

Fig. 10: Correlation plots of metal oxides obtained with SEM

PXRF qualitative analysis of pre-concentrated ore (Table 4) indicated that the NIR-sensor-based sorting and classification produce fractions with characteristic metal concentrations. It was found that the copper grade increases sharply according to the classification from waste to middling to product. With calcium, the inverse trend was observed: the waste fractions contain the highest calcium concentration while the product fraction contained the lowest calcium. The grades of all the selected elements follow a different pattern. With iron, the metal dominated the middling fraction with ranged concentration of (49.1 to 55.6% concentration) which is higher than the product fraction (32.9 to 42.2% concentration) which, in turn, is greater than the waste fractions. This pattern is also observed for nickel and cobalt. The inverse pattern, where the middling ranked lowest and the waste grade is highest, occurs for manganese, barium, potassium, silicon, titanium, and the residue fractions. With phosphorus, the product and middling grades are similar with a higher waste grade. The opposite is true for vanadium and chromium. In terms of elemental grade in the different size fractions, it was observed that in the product size fractions, an increase in copper concentration with increasing particle size was the case (from −63+45 µm to −180+125 µm). The same was observed for both the middling and waste fractions. The opposite trend applies to iron, potassium and the residue fractions in the product size fractions.

The trend of increasing iron grade with decreasing particle size is also observed in the middling and waste fractions. Of particular importance is the concentration of calcium and silicon as the major constituent of the minerals. The concentration of these metals expectedly, is higher in the middling and waste categories, which signifies a difference in metal grade of copper. Therefore, it is observed that there is a positive correlation between elemental concentration and host minerals. For instance, the concentration of copper, iron and calcium is a reflection of their abundances in the following minerals: Cu (chrysocolla, malachite and cuprite), Fe (hematite and chlorite) and Ca (feldspars, calcite and ankerite). This pattern is a clear indication that the mineralogy of the ores has influence in determining the outcome of the ore behaviour.

Table 4: PXRF Qualitative analysis of sensor-base pre-concentrated ore (Wt. %)

Sample Category	Particle size Range (µm)	Cu	Ni	Co	Fe	Mn	Ba	Cr	V	Ti	Ca	K	Al	P	Si	Residue
Product	−180+125	1.83	0.02	0.02	32.9	0.06	0.05	0.04	0.04	0.26	0.23	2.21	2.1	0.28	7.9	51.9
	−125+90	1.82	0.01	0.03	36.2	0.05	0.05	0.04	0.04	0.26	0.22	2.12	2.3	0.27	7.9	48.5
	−90+63	1.73	0.01	0.03	38.2	0.05	0.03	0.04	0.04	0.27	0.24	2.05	2.2	0.27	7.8	46.9
	−63+45	1.56	0.01	0.04	42.2	0.05	0.02	0.04	0.04	0.25	0.25	1.81	2.1	0.27	7.5	43.7
Middling	−180+125	0.36	0.02	0.02	49.1	0.00	0.03	0.04	0.04	0.09	1.68	1.01	1.5	0.27	5.3	40.1
	−125+90	0.33	0.03	0.05	52.8	0.00	0.02	0.04	0.04	0.08	1.60	0.93	1.5	0.26	5.1	37.1
	−90+63	0.34	0.03	0.06	53.3	0.00	0.02	0.04	0.04	0.09	1.61	0.90	1.5	0.27	5.0	36.6
	−63+45	0.32	0.04	0.06	55.6	0.11	0.03	0.04	0.04	0.09	1.55	0.82	1.6	0.26	4.8	34.7
Waste	−180+125	0.07	0.03	0.00	8.10	0.14	0.09	0.02	0.02	0.27	4.66	3.74	2.3	0.36	11.0	68.8
	−125+90	0.07	0.00	0.00	8.20	0.13	0.10	0.02	0.03	0.27	5.25	3.83	2.2	0.38	10.0	68.4
	−90+63	0.07	0.00	0.00	9.20	0.13	0.09	0.02	0.03	0.28	5.94	3.76	2.1	0.38	10.0	67.2
	−63+45	0.07	0.00	0.00	10.0	0.13	0.09	0.02	0.03	0.30	6.12	3.86	2.3	0.39	10.0	65.9

The ICP-MS was used to determine some metals (copper, zinc, manganese, cobalt and nickel), Table 5. With ICP-MS it was found that, the copper grade increases sharply with a decrease in particle sizes (–45 to –125+90 µm) in the product and middling. This is to be expected due to increase in surface area with decreasing particle sizes. This suggests that the higher specific area of finer particles makes these more amenable for dissolution due to effective interaction with chemicals for reactions to occur. The same trend of increasing metal concentration with decreasing particle fraction was observed using the ICP-MS. With manganese, nickel, cobalt and zinc, the concentration is lower than that observed in the product. Iron was not analysed using this technique due to its significant concentrations in the classified ore as determined by other methods analysis. Concentration of Fe in the ore is above the range limit of the ICP-MS, thus in each case the determination would require huge dilutions which cannot be accurately equated in relation to the concentration of the other metals.

Table 5: Metal grades determined with ICP-MS

Sample category	Particle size range (µm)	Cu (wt. %)	Zn (ppm)	Mn (ppm)	Co (ppm)	Ni (ppm)
Product	−125+90	1.04	0.01	0.04	0.00	0.00
	−90+63	1.70	0.01	0.05	0.00	0.00
	−63+45	1.79	0.02	0.06	0.03	0.01
	−45	1.97	0.02	0.06	0.03	0.01
Middling	−125+90	0.70	0.01	0.01	0.01	0.00
	−90+63	0.72	0.02	0.02	0.01	0.00
	−63+45	1.01	0.02	0.02	0.03	0.02
	−45	1.10	0.02	0.03	0.04	0.02

The ICP-MS reveals that the pattern of metal concentration was consistent across the entire size fraction. The observation could be due to aqua regia digestion before ICP-MS determination which releases the metals locked up in the complex ore matrix. This will serve as a guide toward establishing a relationship between particle size fractions and metal concentration in ores.

Conclusion

The mineralogical and chemical analysis of sensor-base pre-concentrated copper ores was carried out. It was found that all the results obtained correlated indicating good correlation of analyses. The mineralogy of the ore by QEMSCAN® and XRD shows that the copper ore samples consisted of different minerals which are broadly divided into for classes as silicate, oxide, phosphate, carbonate and oxide. The three main copper-bearing minerals in the ore are chrysocolla, malachite and cuprite. Chrysocolla was determined to be the major copper-bearing mineral and the bulk ore is a silicate oxide. SEM analysis of the classified ore indicated that copper is finely disseminated in the ore. The ore mineral chemistry also revealed a positive correlation suggesting good ore analysis. PXRF results of size fractions indicated higher content of metals compared to particle samples: This is an indication that liberation of the classified ore led to exposure of the ore for effective determination. Results of the metals determined by the PXRF quantitative technique of size fractions and aqua regia digestion, followed by ICP-MS metal determination showed that both instruments in some cases either overestimated or underestimated the concentrations of the metals. This suggests that the concentration of metals in copper ores cannot be effectively determined using one

particular technique. The observation could be caused by the differences in the methods of sample preparation and or measurement. In general, the results of the investigation are in accordance with the classification thus corroborating the pre-concentration strategy adopted. The result of this investigation suggests the potential of the application of the sensor base sorting technique for copper pre-concentration of the ore samples obtained from the mine locations.

Conflict of Interest

Authors declare that there is no conflict of interest related to this paper.

References

Amos IA, Shekwonyadu I & Hylke JG 2020. Selective leaching of copper from near infrared sensor-based pre-concentrated copper ores. *Physicohem. Probl. Miner. Process.*, 204-218.

Amos IA, Alafara AB, Bako DA, Janet IO & Kuranga IA 2017. Leaching kinetics of near infrared sensor-based pre-concentrated copper ores by sulphuric acid. *Physicochem. Probl. Miner. Process*, 53(1): 489-501.

Anderson JCO, Rollinson GK, Snook B, Herrington R & Fairhurst JR 2009. Use of QEMSCAN® for the characterization of Ni-rich and Ni-poor goethite in laterite ores. *Miner Engr.*, 22: 1119-1129.

Baba AA, Ayinla KI, Adekola FA, Bale RB, Ghosh MK, Alabi AG & Folorunso IO 2013. Hydrometallurgical application for treating a Nigerian chalcopyrite ore in chloride medium: Part I. Dissolution kinetics assessment. *Int. J. Min., Metallurgy, and Mat.*, 20(11): 1021-1028.

Biswas AK & Davenport WG 2013. Extractive Metallurgy of Copper: International Series on Materials Science and Technology. Elsevier.

Celio P 2003. Near infrared spectroscopy: Fundamentals, practical aspects and analytical applications. *J. Braz. Chem. Soc.*, 14(2): 198-219.

Dalm M, Michael WNB, Frank JA, Van R & Jack HLV 2014. Application of near infrared spectroscopy to sensor based sorting of porphyry copper ore. *Minerals Engineering*, 58: 7-16.

El-Taher A 2012. Elemental analysis of granite by instrumental neutron activation analysis (INAA) and X-ray fluorescence analysis (XRF). *J. Appl. Radiation and Isotopes.*, 70: 350-354.

Gaydon JW 2011. The Application of a Near-infrared Sensor to the Sorting of Minerals. Doctoral thesis Camborne School of Mines, University of Exeter, Penryn Campus.

Gottlieb P, Wilkie G, Sutherland D, Ho-Tun E, Suthers S, Perera K, Jenkins B, Spencer S, Butcher A & Rayner J 2000. Using quantitative electron microscope for process mineralogy applications. *JOM*, 52(4): 24-25.

Helle S, Kelm U, Barrientos A, Rivas P & Reghezza A 2005. Improvement of mineralogical and chemical characterization to predict the acid leaching of geometallurgical units from Mina Sur, Chuquicamata, Chile. *Miner. Eng.*, 18: 1334–1336.

Hillier S 2000. Accurate quantitative analysis of clay and other minerals in sandstones by XRD: Comparison of a Rietveld and a reference intensity ratio (RIR) method and the importance of sample preparation. *Clay Minerals.*, 35: 291-302.

Iyakwari S, Glass HJ & Kowalczuk PB 2013. Potential for near infrared sensor-based sorting of hydrothermally-formed minerals. *J. Near Infrared Spectroscopy*, 21(3): 223-229.

Iyakwari S 2014. Application of Near infrared Sensors to Minerals Pre-concentration. Doctoral thesis Camborne School of Mines, University of Exeter, Penryn Campus.

Iyakwari S, Glass HJ, Gavyn KR & Kowalczuk PB 2016. Application of near infrared sensors to preconcentration of hydrothermally-formed copper ore. *Miner. Engr.*, 85: 148-167.

Kalichini MS, Goodall WR, Paul EM, Prinsloo A & Chongo C 2017. Applied mineralogy at Kansanshi mine - proof of the concept of on-site routine process mineralogy for continuous improvement of plant operations. *Proceed. Process Mineralogy* 17, Cape Town. Minerals Engineering International, Falmouth, UK, pp. 1-10.

Liu W, Tang MT, Tang CB, He J, Yang SH & Yang JG 2010. Dissolution kinetics of low grade complex copper ore in ammonia-ammonium chloride solution. *Transactions of the Nonferrous Metals Society of China.*, 20(5): 910-917.

Neighbour M 2010. Tantalum and Niobium Mineralogy and Recovery from Kaolinised Cornish granite, Doctoral thesis Camborne School of Mines, University of Exeter.

Oscar B, Maria CH, Evelyn M, Damian N, Victor Q & Yuri Z 2019. Copper dissolution from black copper ore under oxidizing and reducing conditions. *Metals*, 9(799): 1-12.

Pirrie D & Rollinson GK 2011. Unlocking the applications of automated mineral analysis. *Geology Today.*, 27(6): 226-235.

Queralt M, Ovejero ML, Carvalho AF, Marques & Llabres JM 2005. Quantitative determination of essential and trace element content of medicinal plants and their infusions by XRF and ICP techniques. *X-Ray Spectrom.*, 34: 213–217.

Reed SJB 2005. Electron Microprobe Analysis and Scanning Electron Microscopy in Geology. Cambridge University Press.

Sabins FF 1999. Remote sensing for mineral exploration. *Ore Geol. Rev.*, 14: 157–183.

Salter JD & Wyatt NPG 1991. Sorting in the minerals industry: past, present and future. *Miner. Eng.*, 4: 779–796.

Thompson AJB, Hauff PL & Robitaille AJ 1999. Alteration mapping in exploration: application of short-wave infrared (SWIR) spectroscopy. *Soc. Econ. Geol. Newsletter*, 39: 15–27.

Helaluddin ABM, Reem SK, Mohamed A & Syed AA 2016. Main analytical techniques used for elemental analysis in various matrices. *Tropical J. Pharmac. Res.*, 15(2): 427-434.

Little L, Mclennan Q, Prinsloo A, Muchima K, Kaputula B, & Siame C 2018. Relationship between ore mineralogy and copper recovery across different processing circuits at Kansanshimine. *J. S. Afr. Inst. Min. Metall.*, 118(11).

Whiteman E, Lotter NO & Amos SR 2016. Process mineralogy as a predictive tool for flow sheet design to advance the Kamoa project. *Minerals Engr.*, 96–97: 185-193.

Wotruba H & Riedel F 2005. Ore preconcentration with sensor-based sorting. *Aufbereitungs Technik,*, 46(5): 4–13.

Wotruba H, Robben MR & Balthasar D 2009. Near-infrared sensor-based sorting in the minerals industry. In Proc. Conference in minerals engineering. Lulea Technical University, Lulea (Sweden), pp. 163–176.

Zhou X, Liu D, Bu H, Deng L, Liu H & Yuan D 2018. XRD-based quantitative analysis of clay minerals using reference intensity ratios, mineral intensity factors, Rietveld, and full pattern summation: methods: A critical review. *Solid Earth Science*, 3: 16-29.